Lead–Calcium Hydroxyapatite: Cation Effects in the Oxidative Coupling of Methane

Yasuyuki Matsumura,[1] Shigeru Sugiyama,* Hiromu Hayashi,* and John B. Moffat[2]

*Department of Chemistry and the Guelph–Waterloo Centre for Graduate Work in Chemistry, University of Waterloo, Waterloo, Ontario, Canada N2L 3G1; and *Department of Chemical Science and Technology, the University of Tokushima, Minamijosanjima, Tokushima 770, Japan*

The properties of calcium hydroxyapatite and a number of lead–calcium hydroxyapatites are examined, and their activities in the conversion of methane with nitrous oxide and oxygen as oxidants are compared. The introduction of a small quantity of lead considerably alters both the conversion of methane and the selectivities to the various products. The introduction of lead appears to assist in the stabilization of methyl radicals, while the formation of ensembles of surface lead atoms brings methyl radicals into sufficiently close proximity so as to induce bonding between the radicals and formation of ethane. © 1995 Academic Press, Inc.

INTRODUCTION

Potential processes for the conversion of natural gas to value-added products continue to attract the attention of scientists working on heterogeneous catalysis (1). Although a wide variety of catalysts has been tested for the oxidative coupling of methane, the conversion of methane and the selectivities to hydrocarbons containing two or more carbon atoms are less than desirable under the present economic conditions (2). The many studies which have been reported have, however, provided considerable information concerning the surface and catalytic properties of the solids examined as potential catalysts and the mechanisms of the methane conversion processes.

Hydroxyapatite [$Ca_{10}(PO_4)_6(OH_2)$] is an inorganic solid, found naturally in hard tissues such as bone and teeth. A number of the most interesting characteristics of hydroxyapatite were described almost 30 years ago (3). It is well known that the preparation of pure hydroxyapatite with a Ca/P ratio of 1.67 is difficult since small deviations from the stoichiometric composition lead to the formation of other calcium phosphates such as tricalcium phosphate (4, 5). Hydroxyapatite does not readily lose hydroxyl groups, and the lattice is believed to be stable up to 1000°C (6). Temperatures above 1500°C convert the hydroxyapatite to tri- and tetracalcium phosphate.

As a consequence of its biological importance, a considerable number of X-ray diffraction and transmission electron microscopic (TEM) studies have been reported (7–11). Recent work has shown that hydroxyapatite is converted to the high temperature form of tricalcium phosphate [α-$Ca_3(PO_4)_2$] in the ion-beam of TEM (12), apparently due to either decomposition of the hydroxyapatite or the release of hydrogen.

Although hydroxyapatite has been well studied by X-ray diffraction and transmission electron microscopy, until recently there have been no reports on its surface structure. Siperko and Landis (13) have now shown by the application of atomic force microscopy that the crystal surface structure is highly ordered with atomic spacings of 0.68 and 0.43 nm.

Hydroxyapatite has a hexagonal structure constructed from columns of Ca and O atoms which are parallel to the hexagonal axis. Three oxygen atoms of each PO_4 tetrahedron are shared by one column, with the fourth oxygen atom attached to a neighboring column. The hexagonal unit cell of hydroxyapatite contains 10 cations located on two sets of nonequivalent sites, 4 on site [1] and 6 on site [2]. The calcium ions on site [1] are aligned in columns, while those on site [2] are in equilateral triangles centered on the screw axes. The site-[1] cations are coordinated to six oxygen atoms belonging to different PO_4 tetrahedra and also to three oxygen atoms at a large distance. The site-[2] cations are found in cavities in the walls of the channels formed between the cations and O atoms. The hydroxyl groups are situated in these channels and probably form an approximately triangular coplanar arrangement with the Ca ions.

Not surprisingly, a number of substitutions are possible for the cations and anions contained within hydroxyapatite (14–19). These substitutions may alter the crystal-

linity, lattice parameters, morphology, and stability of the structure. As expected from the difference in ionic radii, the substitution of lead for calcium in the hydroxy-apatite structure produces an increase in the size of the unit cell (18, 19). Although the hydroxyapatite structure contains two nonequivalent cation sites, there is strong evidence that, for compositions of less than 50% lead atoms, the latter occupy mostly site [2]. Lead substitution for calcium in the hydroxyapatite structure also leads to a shift of the IR bands characteristic of the PO_4^{3-} internal modes to lower frequencies. Although this shift is larger for lead compositions greater than 50 at.%, a shift of the OH stretching mode to lower frequencies is observed as lead is added up to 50 at.%.

In the present work, calcium and lead–calcium hydroxyapatites, synthesized from aqueous solution, the latter with lead/calcium compositions up to 3/7, are examined as catalysts for the oxidative coupling of methane at 700°C with either oxygen or nitrous oxide as oxidant. In the oxidative coupling, dioxygen has been usually used as the oxidant, while nitrous oxide is frequently used as an oxidant for the partial oxidation of methane to methanol or formaldehyde (20). Although the coupling of methane with nitrous oxide is not economical, studies of the reaction with nitrous oxide can provide information on the nature of active surface oxygen species. Nitrous oxide has been found to be an effective oxidant for the methane coupling with Li/MgO (21) and Sm_2O_3 (22), and atomic oxygen species such as O^- which are produced from the dissociation of this oxidant have been suggested to be the active forms of oxygen in this process.

Catalysts containing lead ions often show excellent activity for methane coupling (23–33). Calcium ions in hydroxyapatite $[Ca_{10-z}(HPO_4)_z(PO_4)_{6-z}(OH)_{2-z}; 0 \leq z \leq 1]$ can be replaced by lead (34) and the lead-modified apatite catalyzes the oxidative coupling of methane with high

selectivity to C_{2+} compounds at temperatures as low as 700°C (35), while lead oxide supported on a basic compound such as magnesium oxide yields similar selectivity at ca. 750°C or above (31).

It is known that lead–calcium hydroxyapatite can be synthesized from aqueous solutions of calcium, lead, and phosphate (19). In the apatite, lead ions are the constituents of the structure; hence the ions are considered to be well dispersed in the sample. While it has been proposed that the lattice oxygen of lead oxide is involved in methane oxidation (36), the active oxygen species in the lead–calcium apatite have not been identified.

EXPERIMENTAL

Calcium and lead–calcium hydroxyapatites were prepared from $NaHPO_4 12H_2O$ (BDH, AnalaR), $Ca(CH_3COO)_2H_2O$ (Baker, Analyzed), and $Pb(CH_3COO)_2 3H_2O$ (BDH, ACS) according to the method described in Ref. (19). The resulting solids were heated in air at 500°C for 3 hr. The chemical compositions of the prepared samples were determined by atomic absorption spectrometry for cations and by ion chromatography for anions. The values for the samples ($CaAp$, $Pb_{0.01}Ap$, $Pb_{0.02}Ap$, $Pb_{0.05}Ap$, $Pb_{0.06}Ap$, $Pb_{0.09}Ap$, $Pb_{0.11}Ap$, and $Pb_{0.30}Ap$) are given in Table 1. Formation of hydroxyapatite structure was confirmed by recording the X-ray diffraction (XRD) patterns for these samples (37). No peaks other than those of hydroxyapatite were observed.

Methane conversion was performed in a conventional fixed-bed continuous flow reactor operated under atmospheric pressure. The reactor consisted of a quartz tube of 8 mm id and 35 mm length sealed at each end to 4-mm-id quart tubes. The catalyst was sandwiched with quartz wool plugs whose contribution to the reaction was negligible. The reactants were diluted with helium gas and the

TABLE 1
Composition of Hydroxyapatites

| Sample | Molar ratio in sample | | | Content of Na (wt%) | XRD[a] I_{TCP}/I_{apa} | BET[b] $(m^2 g^{-1})$ |
	Pb/(Pb + Ca)	Ca/P	Pb/P			
CaAp	0.000	1.52	0.00	0.8	0.44	10.1
$Pb_{0.01}Ap$	0.010	1.70	0.02	0.8	0.73	12.9
$Pb_{0.02}Ap$	0.022	1.62	0.04	0.7	0.64	15.5
$Pb_{0.05}Ap$	0.053	1.56	0.09	0.5	1.25	13.8
$Pb_{0.06}Ap$	0.063	1.55	0.10	0.7	0.30	13.6
$Pb_{0.09}Ap$	0.086	1.55	0.14	0.6	0.15	15.2
$Pb_{0.11}Ap$	0.106	1.54	0.18	0.5	0.26	14.8
$Pb_{0.30}Ap$	0.300	1.27	0.56	0.3	2.22	10.7

[a] I_{TCP}, peak intensity attributed to β-tricalcium phosphate at 30.8° in 2θ; I_{apa}, peak intensity attributed to hydroxyapatite at 31.5°; samples were obtained after the reactions shown in Fig. 1.

[b] BET surface area of samples after reactions shown in Fig. 3.

total flow rate was 0.9 dm³ hr⁻¹. Catalysts (0.05–0.30 g) were preheated in the flow of oxygen (6 kPa) diluted with helium (total flow rate, 0.6 dm³ hr⁻¹) at 700°C for 1 hr. The reactants and products were analyzed with an on-stream gas chromatograph equipped with a TCD. Two columns, one Porapak T (5.4 m) or HeySep Dip (5.4 m), the other molecular sieve 5A (0.4 m), were used in the analyses. The conversion and selectivities were calculated on the basis of the amounts of reaction products formed as determined by the GC analysis.

The surface areas of the catalysts were measured by the conventional BET nitrogen adsorption method.

Surface analyses by XPS were carried out using a Shimadzu ESCA-1000AX spectrometer. The samples were mounted on a sample holder in air and set into the spectrometer. After measurement argon-ion etching of the sample was carried out (2 kV, 1 min), and the spectra were measured again after etching. Charge correction of the XPS data was accomplished by assuming that the binding energy of the C 1s peak was at 284.6 eV.

RESULTS

Methane Coupling with Nitrous Oxide

With nitrous oxide as oxidant the oxidative coupling of methane at 700°C on lead–calcium hydroxyapatite catalysts produced conversions which increased with the lead content up to a Pb/(Pb + Ca) ratio of 0.05 but decreased for further increases in the ratio (Fig. 1). Concomitantly, the C_{2+} selectivities showed similar behavior for low lead contents, while the selectivities to CO and CO_2 decreased. All three of these selectivities remained essentially constant at approximately 90% for Pb/(Pb + Ca) greater than 0.05. The selectivities to C_2H_6 and C_2H_4 reached plateaus at Pb contents between 0.022 and 0.05,

but for further increases in Pb content they increased and decreased, respectively. The conversion and C_{2+} selectivities obtained with CaAp were lower than those obtained with any of the PbAp samples studied and the CO_2/ CO ratio found with this catalyst was approximately 1.5. No hydrogen was produced with any of these samples.

Since the decomposition of nitrous oxide to dinitrogen and dioxygen is a thermodynamically spontaneous reaction at 700°C, experiments were carried out to examine this decomposition on the lead–calcium hydroxyapatite catalysts in the presence and absence of methane. The formation of dioxygen was observed at all compositions of lead–calcium hydroxyapatite examined.

The conversion of the oxidant, nitrous oxide, at 700°C showed qualitatively similar behavior to that observed with methane (Fig. 2). In the absence of methane the conversion of N_2O increased to a maximum of approximately 38% at a Pb/(Pb + Ca) value of 0.06 and, with further increase in the lead content, decreased. The conversions of N_2O observed in the presence of methane were higher than those in its absence for all catalyst compositions studied. In the presence of methane a maximum in N_2O conversion was again observed but at a higher value of 48% and at a lead content of 0.05.

The XRD patterns of the catalysts after use in the methane coupling with nitrous oxide reaction contained peaks at 2θ values of 30.8° and 31.5° which are attributed to β-tricalcium phosphate and hydroxyapatite, respectively. The ratio of the intensities of these peaks show two maxima, for $Pb_{0.05}Ap$ and $Pb_{0.30}{}^{Ap}$ (Table 1). No peaks attributed to lead oxides were observed, although a peak assigned to lead orthophosphate was found at 22.3° in the pattern for $Pb_{0.30}Ap$. The patterns were very similar to those recorded after the pretreatment at 700°C for 1 hr and prior to use in the reaction.
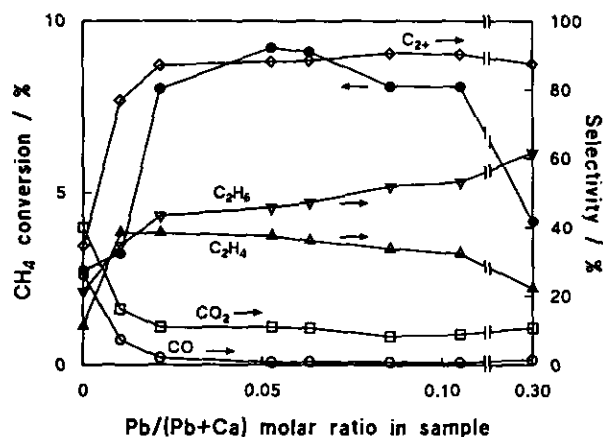

FIG. 1. Oxidative coupling of methane with nitrous oxide over lead–calcium hydroxyapatite. Reaction conditions: reaction temperature, 700°C; catalyst, 0.30 g; partial pressure of methane, 29 kPa; nitrous oxide, 7 kPa; total flow rate, 0.9 dm³ hr⁻¹; time on stream, 3 hr.
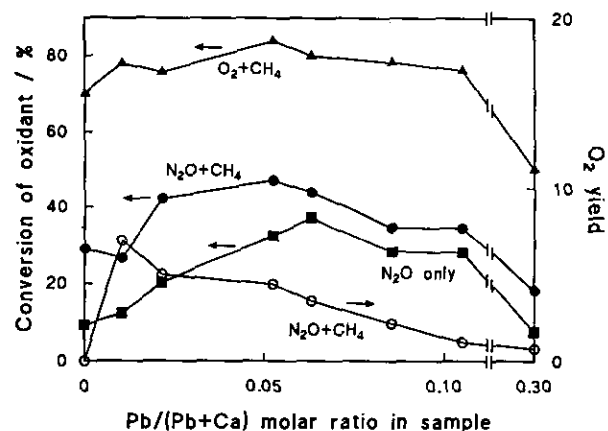

FIG. 2. Conversion of oxidant in oxidative coupling of methane over lead–calcium hydroxyapatite. Reaction conditions: reaction temperature, 700°C; catalyst, 0.30 g; partial pressure of methane (if present) 29 kPa; nitrous oxide (if present), 7 kPa; dioxygen (if present), 4 kPa; total flow rate, 0.9 dm³ hr⁻¹; time on stream, 3 hr.

Methane Coupling with Dioxygen

The conversion of methane and the selectivities to the various products with dioxygen as oxidant followed trends similar to those observed with nitrous oxide (Fig. 3). In the former case, however, the conversion was significantly higher for all catalyst compositions and the maximum appeared at a lead content of 0.10. With oxygen, the C_{2+} selectivities did not exceed 80%. No formation of hydrogen was observed except in the reaction on CaAp. In this latter case the selectivity to carbon monoxide was approximately four times that to CO_2, in sharp contrast with the CO/CO_2 ratio of approximately 0.5 obtained with nitrous oxide as oxidant. It has previously been shown that, in the absence of lead, nonstoichiometric calcium hydroxyapatite generates a high selectivity to carbon monoxide in the oxidation of methane with dioxygen (35). For all catalyst compositions the conversion of oxygen in the presence of CH_4 substantially exceeds the corresponding conversion of nitrous oxide (Fig. 2). It should be noted that the partial pressure of dioxygen in these experiments was approximately half that of the nitrous oxide fed in the reactions shown in Fig. 1. The values of the BET surface area for these samples after the reaction were described in Table 1.

Ethane Dehydrogenation over Lead–Calcium Hydroxyapatite

The formation of ethylene in the oxidative coupling of methane is believed to result predominantly from the further dehydrogenation of ethane produced in the reaction. Since this process may also consume oxidants, different oxidants are expected to produce dissimilar results in the reaction.
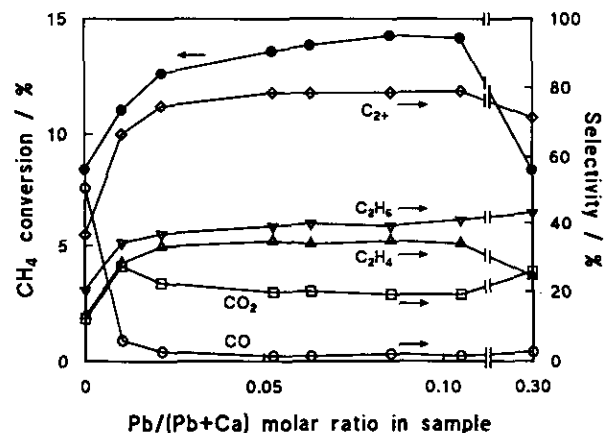

FIG. 3. Oxidative coupling of methane with dioxygen over lead–calcium hydroxyapatite. Reaction conditions: reaction temperature, 700°C; catalyst, 0.30 g; partial pressure of methane, 29 kPa; dioxygen, 4 kPa; total flow rate, 0.9 dm³ hr⁻¹; time on stream, 3 hr.

With nitrous oxide as an oxidant ethylene was the predominant product formed from ethane over lead–calcium apatites while carbon monoxide, carbon dioxide, methane, and water were also produced (Table 2). An appreciable amount of hydrogen was detected during the reaction. Little or no oxygen was produced in the reaction.

Although the conversion of methane with dioxygen was significantly higher than that with nitrous oxide, the conversion of ethane with dioxygen as an oxidant was generally lower than that with nitrous oxide while the selectivity to ethylene with dioxygen is somewhat higher (see Table 2). The differences in these latter selectivities can primarily be associated with differences in those to CO_2, rather than to CO. Formation of a small amount of hydrogen was also observed.

TABLE 2
Ethane Dehydrogenation over Lead–Calcium Hydroxyapatites[a]

| Catalysts | Oxidant | Conversion (%) | | Selectivity (%) | | | | H_2/C_2H_4[b] |
		C_2H_6	Oxidant	C_2H_4	CH_4	CO	CO_2	
$Pb_{0.01}Ap$	N_2O	25.1	69	84.3	4.1	3.0	8.7	0.3
$Pb_{0.02}Ap$	N_2O	31.5	96	80.8	4.5	3.6	11.0	0.2
$Pb_{0.05}Ap$	N_2O	28.9	92	82.7	3.8	2.7	10.8	0.1
$Pb_{0.01}Ap$	O_2	19.5	56	86.7	4.0	3.7	5.6	0.1
$Pb_{0.02}Ap$	O_2	21.1	57	89.1	3.4	2.5	5.1	0.04
$Pb_{0.05}Ap$	O_2	32.9	89	87.7	3.9	2.8	5.5	0.1
$Pb_{0.01}Ap^c$	None	6.0		97.7	2.3			1.0
$Pb_{0.02}Ap^c$	None	6.0		97.9	2.1			1.0
$Pb_{0.05}Ap^c$	None	7.0		97.9	2.1			1.0

[a] Reaction conditions unless otherwise noted: reaction temperature, 700°C; amount of catalyst, 0.05 g; partial pressure of ethane, 15 kPa; nitrous oxide (if present), 7 kPa; dioxygen (if present), 4 kPa; total flow rate, 0.9 dm³ hr⁻¹; time on stream, 3 hr.

[b] Molar ratio of H_2/C_2H_4 in products.

[c] Amount of catalyst, 0.15 g.

TABLE 3

Binding Energies of the Surface Elements
on Lead–Calcium Hydroxyapatites

| Sample | Binding energy (eV) | | | | C^a |
	P $2p$	Pb $4f_{7/2}$	Ca $2p_{3/2}$	O $1s$	Pb (mole %)
CaAp	133.5		347.6	531.7	0
Pb$_{0.01}$Ap	133.4	139.0	347.3	531.3	2
Pb$_{0.02}$Ap	133.7	139.6	347.6	531.6	3
Pb$_{0.06}$Ap	133.7	139.5	347.7	531.7	5
Pb$_{0.11}$Ap	133.4	139.1	347.7	531.5	6
Pb$_{0.30}$Ap	133.8	139.5	347.9	531.7	8

^{a} Surface concentration of Pb.

In order to estimate the contribution of the dehydrogenation of ethane without oxidants to the oxidative dehydrogenation, the conversion of ethane in the absence of oxidant was examined. Decomposition of ethane to ethylene and hydrogen can take place at 700°C (the equilibrium yield of ethylene is calculated as 69% under the present reaction conditions), although, not surprisingly, the conversion of ethane in the absence of an oxidant was considerably lower than that in its presence. The formation of appreciable amounts of ethylene and hydrogen was observed over lead–calcium hydroxyapatite. A small amount of methane was also detected.

Analyses by XPS

In order to characterize the surface of the lead–calcium hydroxyapatites, XPS analyses were carried out for the samples pretreated at 700°C for 1 hr under the same pretreatment stream of the reaction. No significant differences in binding energies of Pb $4f_{7/2}$, Ca $2p_{3/2}$, P $2p$, and O $1s$ were observed among the samples (Table 3). No signifi-
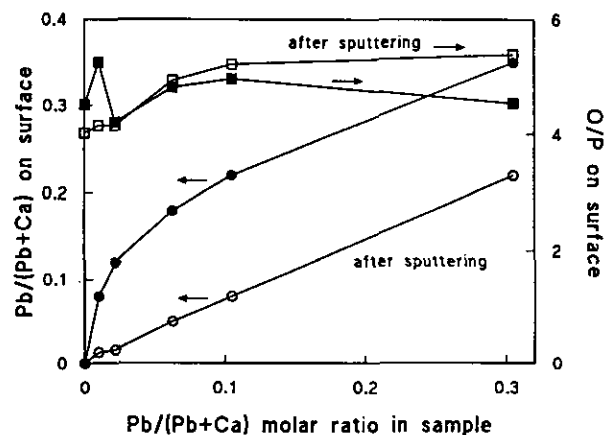

FIG. 4. Surface composition of lead–calcium hydroxyapatite determined by XPS. The surface composition was determined from the peak intensities of Pb $4f_{7/2}$, Ca $2p_{3/2}$, P $2p$, and O $1s$ using the sensitivity factors 4.786, 1.218, 0.355, and 0.711, respectively.

cant shoulders or other peaks were observed in the spectra (not shown). The surface atomic ratio of Pb/(Pb + Ca) in lead–calcium apatite determined from the peak area was significantly higher than the ratio determined by chemical analyses (Fig. 4, solid circles). The values obtained after argon-ion sputtering for 1 min were similar to the chemical molar ratios (Fig. 4, open circles). The values for the surface atomic ratio of O/P were also determined. The molar ratio of O/P in hydroxyapatite is calculated to be 4.3 from the chemical compositions. The values observed corresponded roughly to the calculated value, but no significant correlation with the lead content of the same was obtained (Fig. 4, squares). The XPS analyses on samples previously employed in the reaction showed little or no change from those shown in Table 3 and Fig. 4.

DISCUSSION

Asami *et al.* reported that the reaction rate of the coupling of methane on lead oxide supported on magnesium oxide is approximately similar with dioxygen to that found with nitrous oxide, suggesting that the lattice oxygen of lead oxide is the active oxygen species for the reaction (36). Other workers have proposed that the catalytically active sites were those present on the magnetoplumbite phase (38), while Marcelin and co-workers have proposed that isolated sites of PbO could be responsible for the activity (39). Most recently, Park and Chong (40) have suggested that the activity should be attributed to lead aluminate formed on a lead oxide–alumina catalyst.

The present work demonstrates that the introduction of lead into the calcium hydroxyapatite catalyst significantly enhances the conversion of methane and the selectivities to C_2H_4 and C_2H_6. In addition, with the lead–calcium hydroxyapatites dioxygen is significantly more active than nitrous oxide. Consequently both the activity and selectivities are dependent upon the presence of lead, in whatever form, as well as the nature of the oxidant. This suggests that the mechanism on the present catalysts is dissimilar from that on lead oxide. Further, although β-tricalcium phosphate and, presumably, lead orthophosphate are present in the structure, there is no evidence for the formation of lead oxide. It is known that lead orthophosphate catalyzes the oxidative coupling of methane, but the C_2 selectivity is not high at 740°C (51% at a methane conversion of 9% with a reaction stream containing 66 kPa of methane and 8 kPa of dioxygen) (41) while more recent work at a reaction temperature of 775°C produced a selectivity of 82% (42).

The XRD data provide evidence for significant quantities of tricalcium phosphate in the bulk of the lead–calcium hydroxyapatites and particularly for Pb$_{0.05}$Ap and Pb$_{0.30}$Ap for which maxima of I_{TCP}/I_{apa} are noted. How-

ever, the binding energies as measured by XPS show no significant changes as the lead content is increased, suggesting that the surface structure is invariant during changes in the overall composition. In contrast, both the conversion and selectivities obtained with CaAp, in the absence of lead, and the $Pb_{0.30}Ap$ catalyst are significantly different from those observed with the remaining lead–calcium hydroxyapatites. Hence it can be concluded that the surface structure of CaAp is a necessary, but not a sufficient condition for an active and selective catalyst. The source of the changes in the value of I_{TCP}/I_{apa} for lead–calcium apatite after the methane reaction (Table 1) is not clear, but it is noteworthy that the apatites containing lead are often converted, at least partially, to tricalcium phosphate at temperatures in excess of 500°C (18). The extent of this transformation could be influenced by the water produced in the reaction or impurities such as sodium cations in the solid. Since nonstoichiometric calcium hydroxyapatite is more unstable than the stoichiometric form (35), the ratios of Ca/P and Pb/P in the apatite may also have an influence.

To estimate the surface activity of lead–calcium apatite samples in the methane coupling process, the conversion rate of methane per unit surface area was calculated based on the results shown in Figs. 1–3 and Table 1 (Fig. 5). In methane coupling with either nitrous oxide or oxygen the highest rate of conversion is found with $Pb_{0.05-0.06}Ap$, compositions which show relatively large bulk concentrations for TCP. The trends in the conversion rate with nitrous oxide are similar to those observed in the decomposition of nitrous oxide, suggesting that the decomposition of nitrous oxide is a rate determining step for the methane coupling with nitrous oxide. Formation of dioxygen during the methane coupling with nitrous oxide provides indirect evidence that dioxygen is involved in the reaction even if the oxidant is nitrous oxide.
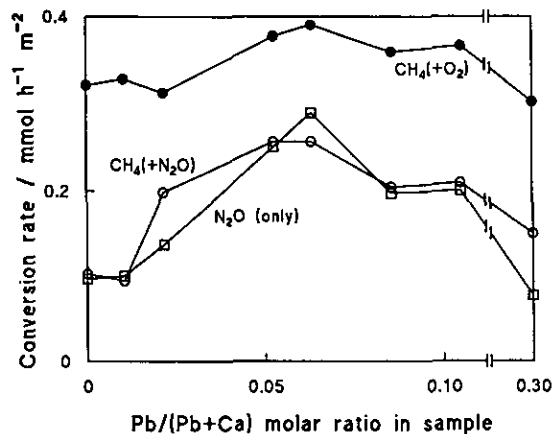

FIG. 5. The surface activity of lead–calcium hydroxyapatite catalysts.

It is, of course, possible that the dioxygen formed from the decomposition of nitrous oxide does not participate in the oxidation of methane. However, since the highest rate of conversion of methane with N_2O itself is found for the $Pb_{0.05-0.06}Ap$ catalysts, it would then be expected that these should produce the maximum yield of dioxygen in the conversion of methane with N_2O. In fact the latter is found with the $Pb_{0.01}Ap$ composition.

With calcium apatite (CaAp) and $Pb_{0.30}Ap$ little or no oxygen is formed in the oxidation of methane with nitrous oxide. In addition, both the rate of conversion of methane with N_2O as oxidant and that of N_2O itself are low. It appears that either the nitrous oxide is directly consumed in the oxidation process and hence the formation of dioxygen during the reaction is suppressed or the decomposition of N_2O is the rate-limiting step. The latter appears to be more probable under the present reaction conditions.

Since the conversion of nitrous oxide in the methane dimerization over the lead–calcium apatite catalysts is higher than that in the decomposition of nitrous oxide (see Fig. 2), a part of nitrous oxide is presumably not consumed in the coupling reaction via dioxygen. Although the conversion of nitrous oxide in the methane coupling is lower than that of dioxygen, the conversion of nitrous oxide in ethane oxidation is higher (see Table 2). Since dioxygen is not formed in the ethane oxidation process, nitrous oxide appears to react directly with ethane. The conversion of nitrous oxide in the ethane oxidation is significantly larger than that in the methane coupling, while the conversion of dioxygen in the ethane oxidation is smaller. Hence, ethane is reactive to nitrous oxide and in the methane coupling ethylene can be formed as a result of reaction between ethane and nitrous oxide. Since dioxygen is more reactive for methane than nitrous oxide, it can be supposed that diatomic oxygen species are effective in the activation of methane. High selectivity to C_{2+} compounds can be produced with a reactant stream of high CH_4/O_2 ratio over hydroxyapatite containing lead (35). Thus, the high selectivity produced with nitrous oxide over lead–calcium apatite catalysts is presumably due, at least in part, to a low surface concentration of the diatomic oxygen species on the solids.

There are, evidently, two factors of particular importance in the interpretation of the present results: (1) the concentration of Pb present on and in the hydroxyapatite structure and (2) the nature of the oxygen species present on and in the catalyst. With either nitrous oxide or oxygen as oxidant the conversion of methane is relatively low in the absence of lead, that is, with the CaAp catalyst. With an increase in the concentration of lead the conversion of methane increases but reaches a plateau and then decreases. Semiquantitatively similar behavior is observed for the C_{2+} selectivity, which increases as

lead is added. However, after reaching a plateau, again at a relatively low concentration of lead, the C_{2+} selectivity remains virtually constant for the higher concentrations of lead employed in the present work.

From the XPS measurements it is evident that the surface concentration of lead is continuously increasing as the bulk concentration increases, although the sharpest increase in the surface concentration occurs for relatively low bulk concentrations. Methyl radicals are generally believed to be formed in the oxidation of methane (1, 23, 24). The relatively low conversions of methane produced by CaAp in the absence of lead suggest that the presence of the latter element is important for the activation of methane and the production of methyl radicals. The marked increase in C_{2+} selectivity with increase in the concentration of lead similarly suggests that lead is a vital element in the coupling of the radicals. The low selectivity to C_{2+} compounds produced by CaAp suggests that the reaction between methyl radicals and an oxidant (or an oxidizing species formed therefrom) takes precedence over the coupling process.

Since lead forms strong highly covalent bonds with carbon (43), it can be expected that lead on the surface of hydroxyapatite is capable of the stabilization of methyl radicals. Presumably the beneficial consequences of such stabilization can only be achieved if the stabilized methyl radicals are able to react with each other, rather than with oxidizing species. Delocalization and migration of the methyl radicals, with retention of their stabilization, appears to be unlikely. Thus the production of ethane from the stabilized free radicals appears to be probable only under conditions such that two free radicals are in close proximity to each other. This will be possible, presumably, only when the surface concentration of lead has achieved a minimum value. This ensemble effect will reach a maximum when the surface concentration of lead has reached a value sufficiently high so as to optimize the pairwise reaction of methyl radicals, and consequently the C_{2+} selectivities would be expected to remain constant for further increases in the surface concentration of lead. However, the sites for activation of methane will, at some concentration of lead, presumably begin to be diminished and the conversion of methane will decrease.

ACKNOWLEDGMENT

REFERENCES

1. A. M. Maitra, *Appl. Catal.* **104**, 11 (1993).
2. J. M. Fox, *Catal. Rev. Sci. Eng.* **35**, 69 (1993).
3. M. I. Kay, R. A. Young, and A. S. Posner, *Nature* **204**, 1050 (1964).
4. M. Jarcho, C. H. Bolen, M. B. Thomas, J. Bo-Bick, F. J. Kay, and R. H. Doremus, *J. Mater. Sci.* **11**, 2027 (1976).
5. K. Yamashita, H. Owada, H. Nakagawa, T. Umegaki, and T. Kanazawa, *J. Am. Ceram. Soc.* **69**, 590 (1986).
6. D. E. C. Corbridge, "The Structural Chemistry of Phosphorus." Elsevier, Amsterdam, 1974.
7. H. Ji and P. M. Marquie, *J. Mater. Sci. Lett.* **10**, 132 (1991).
8. W. J. Landis, J. Moradian-Oldak, and S. Weiner, *Connect. Tissue Res.* **25**, 181 (1991).
9. W. J. Landis and M. J. Glimcher, *J. Ultrastruct. Res.* **63**, 188 (1978).
10. M. I. Kay, R. A. Young and A. S. Posner, *Nature* **204**, 1050 (1964).
11. H. C. W. Skinner, H. T. Hunt and J. Griswold, *J. Phys. E Sci. Instrum.* **13**, 74 (1980).
12. H. Ji and P. M. Marquis, *J. Mater. Sci. Lett.* **10**, 132 (1991).
13. L. M. Siperko and W. J. Landis, *Appl. Phys. Lett.* **61**, 2610 (1992).
14. D. McConnel, "Apatites, Applied Mineralogy," Vol. 5. Springer, New York/Vienna, 1963.
15. J. Lang, *Bull. Soc. Sci. Bretagne* **53**, 95 (1981).
16. G. H. Nancollas, in "Biological Mineralization and Demineralization" (G. H. Nancollas *et al.*, Eds.), Dahlem Workshop Reports, Vol 23, p. 79. Springer, Berlin, 1982.
17. R. Z. Le Geros and J. P. Le Geros, in "Phosphate Minerals" (J. O. Nizidgan and P. B. Moore, Eds.), p. 351. Springer, New York, 1984.
18. A. Bigi, A. Ripamonti, S. Brückner, M. Gazzano, N. Roveri, and S. A. Thomas, *Acta Crystallogr. B* **45**, Sect. 247 (1989).
19. A. Bigi, M. Gandolfi, M. Gazzano, A. Ripamonti, N. Roveri, and S. A. Thomas, *J. Chem. Soc. Dalton Trans.*, 2883 (1991).
20. R. Pitchai and K. Klier, *Catal. Rev. Sci. Eng.* **23**, 13 (1986).
21. H. Yamamoto, H. Y. Chu, M. Xu, C. Shi, and J. H. Lunsford, *J. Catal.* **142**, 325 (1993).
22. K. Otsuka and T. Nakajima, *J. Chem. Soc. Faraday Trans. 1* **83**, 1315 (1987).
23. J. S. Lee and S. T. Oyama, *Catal. Rev. Sci. Eng.* **30**, 249 (1988).
24. Y. Amenomiya, V. I. Birss, M. Goledzinowski, J. Galuszka, and A. R. Sanger, *Catal. Rev. Sci. Eng.* **32**, 163 (1990).
25. G. E. Keller and M. M. Bhasin, *J. Catal.* **73**, 9 (1982)
26. W. Hinsen, W. Bytyn, and M. Baerns, in "Proceedings 8th International Congress Catalysis, Berlin, 1984" Vol. 3, p. 581. Dechema, Frankfurt-am Main, 1984.
27. K. Asami, S. Hashimoto, T. Shikada, K. Fujimoto, and H. Tominaga, *Chem. Lett.* 1233 (1986).
28. H. J. F. Doval, O. A. Scelza, and A. A. Castro, *React. Kinet. Catal. Lett.* **34**, 143 (1987).
29. J. P. Bartek, J. F. Brazdil, and R. K. Grasselli, *Catal. Today* **117**, 3 (1988).
30. K. Aika and T. Nishiyama, in "Proceedings 9th International Congress Calgary, 1988" (M. J. Phillips and M. Ternan, Eds.), Vol. 2, p. 907. Chem. Inst. of Canada, 1988.
31. K. Fujimoto, S. Hashimoto, K. Asami, K. Omata, and H. Tominaga, *Appl. Catal.* **50**, 223 (1989).
32. K. J. Smith, T. M. Painter, and J. Galuszka, in "Preprints 11th Canadian Symp. Catal., Halifax, July 15–18," p. 18, 1990.
33. S. K. Agarwal, R. A. Migone, and G. Marcelin, *J. Catal.* **121**, 110 (1990).
34. T. Suzuki, T. Hatsushika, and M. Miyake, *J. Chem. Soc. Faraday Trans. 1* **78**, 3605 (1982).
35. Y. Matsumura and J. B. Moffat, *Catal. Lett.* **17**, 197 (1993).
36. K. Asami, T. Shikada, and K. Fujimoto, *Bull. Chem. Soc. Jpn.* **64**, 266 (1991).
37. J. V. Smith (Ed.), "Index (Inorganic) to the Powder Diffraction File." ASTM Publication No. PDIS-16i Pa, 1966.

38. G. Wendt, C.-D. Mienecke, and W. Schmitz, *Appl. Catal.* **45,** 209 (1988).
39. S. S. Agarwal, R. A. Migone, and G. Marcelin, *J. Catal.* **121,** 110 (1990).
40. S.-E. Park and J.-S. Chong, *Appl. Catal.* **85,** 117 (1992).
41. J. A. S. P. Carreiro and M. Baerns, *React. Kinet, Catal. Lett.* **34,** 143 (1987).
42. T. Ohno and J. B. Moffat, *Catal. Lett.* **16,** 181 (1992).
43. H. Shapiro and F. W. Frey, "The Organic Compounds of Lead." Wiley, New York, 1968.